J|A|C|S COMMUNICATIONS

Published on Web 06/22/2010

Narrow-Chirality Distributed Single-Walled Carbon Nanotube Growth from Nonmagnetic Catalyst

Zohreh Ghorannevis, Toshiaki Kato,* Toshiro Kaneko, and Rikizo Hatakeyama

Department of Electronic Engineering, Tohoku University, Aoba 6-6-05, Aramaki-Aza, Aoba-Ku, Sendai, Japan

Received April 28, 2010; E-mail: kato12@ecei.tohoku.ac.jp

Abstract: We present the first demonstration of the nonmagnetic catalyzed synthesis of narrow-chirality distributed single-walled carbon nanotubes (SWNTs). Based on the systematic investigation using different combinations of catalyst types (magnetic or nonmagnetic) and chemical vapor deposition (CVD) methods (thermal CVD (TCVD) or plasma CVD (PCVD)), PCVD with the nonmagnetic catalyst under the appropriate H_2 concentration is found to be critical as the methodological element of realizing the narrow-chirality distribution. Electrical measurements of thin film SWNTs produced under the different combinations of catalyst types and CVD methods are also investigated, which reveals the SWNTs grown from the nonmagnetic catalyst with PCVD display the best device performance.

One-dimensional single-walled carbon nanotubes (SWNTs) are potential materials for future nanoelectronics.[1,2] Since the electronic and optical properties of SWNTs strongly depend on their diameter and chiral angle, the selective synthesis of SWNTs with desired chiralities is one of the major challenges in nanotube science and applications.[3−5] Some progress has been made by silica supported CoMo[6] and zeolite supported FeCo[7] catalysts. FeRu[8] and FeNi[9] catalysts have also been developed for narrow chirality distribution. Noticeably, all of these results on the narrow chirality distribution growth have been limited to the case of using magnetic catalysts. Since the existence of the residual ferromagnetic catalyst particles in SWNTs is the main obstacle to the research on intrinsic magnetic properties of SWNTs, the SWNT growth with nonmagnetic catalysts is indispensable. In spite of recent improvements in the SWNT growth with nonmagnetic catalysts,[10−13] the diameter and chirality (n,m) distribution control with the nonmagnetic catalysts is still highly required for the fundamental studies and variety of applications.[14]

Here, we demonstrate a narrow-chirality distributed growth of SWNTs from a Au catalyst. The chirality and diameter distribution are analyzed by photoluminescence excitation/emission (PLE) spectroscopy, UV−vis−NIR absorption spectroscopy, and Raman scattering spectroscopy with multilaser excitation. Based on the systematic investigation using the different combinations of catalyst types (magnetic or nonmagnetic) and chemical vapor deposition (CVD) methods (thermal CVD (TCVD) or plasma CVD (PCVD)), PCVD[15] with the nonmagnetic catalyst under an appropriate H_2 concentration is found to be critical. Electrical characteristics of thin films consisting of SWNTs produced under the different combinations of catalyst types and CVD methods are also investigated, which indicates the device made by SWNTs grown from the nonmagnetic catalyst with PCVD has the highest semiconducting device percentage. The SWNTs growth is carried out with a homemade radio frequency (RF; 13.56 MHz) PCVD system. The same system is used for a TCVD experiment without supplying electrical power to an electrode used for the plasma generation (see Figure S1 in Supporting Information). Figures 1a and 1b show histograms of the intensity ratio of G-peak to D-peak (I_G/I_D) estimated from Raman spectra as functions of RF power (P_{RF}) and electrode−substrate distance (d_{es}), where I_G/I_D gives a quantitative indication of the relative quality of SWNTs. When the radial breathing mode (RBM) in a lower wavenumber region (100−350 cm^{-1}) and G-band split[16] (G^+ and G^-) are clearly observed, we judge that SWNTs are definitely grown. The Au catalyzed SWNT growth with PCVD (Au-PCVD) (Figure 1a) possesses a narrower process window due to the lower catalytic activity of the Au catalyst in comparison with Fe catalzed PCVD (Fe-PCVD) (Figure 1b). The I_G/I_D does not differ between the Au and Fe catalysts under the best conditions (P_{RF} = 50 W and d_{es} = 5 cm). All of the SWNT growth processes with PCVD described hereafter are carried out under the optimum conditions for SWNT growth. PLE mapping[17] is used to assign (n,m) of SWNTs grown from the Au catalyst at different H_2 concentrations (Figure 2a, 2b, and 2c). The total pressure is kept at 50 Pa by adjusting the pumping efficiency of the rotary pump throughout this experiment. Lower H_2 concentrations (0- and 3-sccm) lead to growing larger diameter tubes and more widely (n,m)-distributed tubes with (6,5), (7,5), (7,6), (8,4), (8,6), and (8,7) (Figures 2a and 2b). On the other hand, the 7-sccm H_2 concentration yields the narrowest (n,m) distribution with a dominant peak corresponding to the (6,5) tube. The UV−vis−NIR optical absorbance spectra of Au-PCVD SWNTs grown at the 7-sccm H_2 flow rate show one dominant peak in the first van Hove E_{11} range (900−1400 nm) corresponding to SWNTs with (6,5) chirality (Figure 2d). Since clear metallic SWNT peaks could not be observed in the UV−vis−NIR spectra (Figure 2d), the concentration of metallic SWNTs can be lower than generally grown SWNTs. The RBM in the Raman spectra measured with 632.8 and 778 nm lasers on the same SWNT sample also confirms the growth of the (6,5) SWNTs (Figure 2e). This is the first result showing the narrow chirality distribution of SWNTs grown from a nonmagnetic catalyst.

To elucidate the effects of Au and PCVD on the narrow chirality distribution, other combinations of catalyst types and CVD methods are taken up and systematically investigated. Based on the PLE

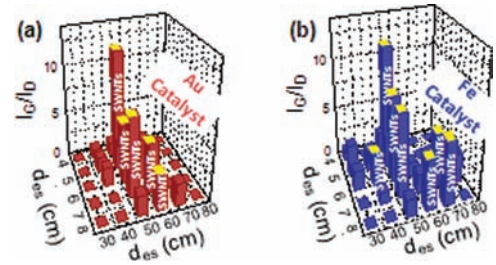

Figure 1. (a) Histogram of I_G/I_D as functions of P_{RF} and d_{es} for SWNTs grown from (a) Au and (b) Fe catalysts with PCVD.

10.1021/ja103362j

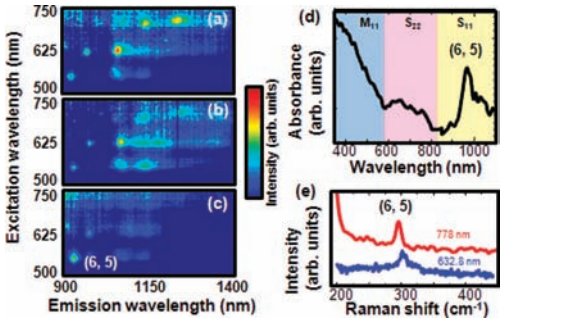

Figure 2. (a) PLE maps of SWNTs from Au catalyst by PCVD at (a) 0-sccm, (b) 3-sccm, and (c) 7-sccm H_2 flow rates, respectively. (d) UV−vis−NIR spectrum of SDBS-dispersed SWNTs grown from Au catalyst at 7-sccm H_2 flow rate and (e) Raman spectra of SWNTs grown from Au catalyst at 7-sccm H_2 flow rate using the excitation laser wavelengths of 632.8 and 778 nm.

analysis, SWNTs grown by the Fe catalyst with PCVD (Fe-PCVD) do not designate any clear dependence in the chirality distribution on the H_2 flow rate, which is fairly broader than that of Au-PCVD (Figure S3a, b, and c in the Supporting Information). This indicates hydrogen-assisted Au catalyzation is one of the critical factors to realize the narrow chirality distribution, which is in good agreement with theoretical predictions. The first-principle calculation by Yazyev et al. reveals that coinage metals such as Cu, Ag, and Au produce narrow chirality distributions.[18] Ding et al. report the SWNT diameter is larger on the surface of Fe, Co, and Ni particles than Cu, Pd, and Au particles because of the different bond energies on the catalyst surface.[19] Following these theoretical models, we can explain the effect of H_2-assisted Au catalyzation on the narrow chirality distirbution as follows. Since the binding energy of hydrocarbons on the Au surface is much weaker than that on the Fe surface, it is difficult in the large-diameter case of the Au catalyst to achieve the cap formation.[19] Additional H_2 also enhances the etching of carbon precursor from the catalyst surface, which strongly suppresses the growth of large diameter SWNTs, and hence the chirality distribution grown from the Au catalyst can be narrower than that from the Fe catalyst. The stability of the cap structure might be a possible reason why the (6,5) tube is dominant in this small diameter Au-PCVD SWNT. The number of cap structures, which satisfy the isolated pentagon rule, is highly limited for small diameter SWNTs, and (6,5) is known to have one of the stable cap structures in this diameter range.[7] The comparison of Au-PCVD and Au-TCVD is also carried out. Although the chirality distribution becomes relatively narrow for the case of SWNTs grown even by Au-TCVD under appropriate H_2 concentrations, it is much broader than that of SWNTs grown by Au-PCVD (Figure S3d, e, and f in the Supporting Information). When we carefully compare the Au-PCVD and Au-TCVD processes, there are two significant differences in the SWNT growth conditions. The first one is the growth temperature. The lower limit of growth temperature with Au-PCVD is 700 °C, which is lower than that of Au-TCVD by 50 °C (Figure S4a, d in the Supporting Information). The second one is an incubation time. The initial SWNT growth is attained at 1 min after the growth substrate is exposed to the plasma in the case of Au-PCVD, whereas 15 min are required for the growth of SWNTs with Au-TCVD. These results suggest that the low temperature and short growth time with Au-PCVD can avoid an aggregation of catalyst particles during the SWNT growth, which suppresses the growth of large diameter SWNTs, resulting in the narrow chirality distribution.[20]

The electrical features are also investigated for the SWNTs grown by Au-PCVD, Fe-PCVD, Au-TCVD, and Fe catalyzed TCVD (Fe-TCVD). As-synthesized SWNTs are dispersed in 1 mL of dimethylformamide (DMF) under ultrasonication for 8 h, followed by spin

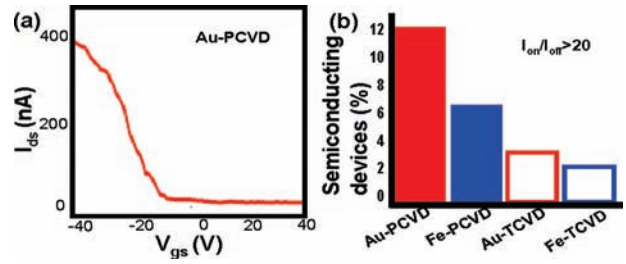

Figure 3. (a) Typical $I_{ds}-V_{gs}$ curve of the thin film FET for Au-PCVD SWNTs. (b) Percentage histogram of semiconducting devices depending on the combinations of catalyst types and CVD methods.

coating between source and drain electrodes of a field effect transistor (FET). To compare the bulk SWNT features, the transport measurements are carried out under the thin film FET configuration including multiconducting channels. We investigate more than 30 such FET devices, and a typical source−drain current (I_{ds}) vs gate bias voltage (V_{gs}) curve is shown in Figure 3a. The percentage of semiconducting devices for each case is calculated in Figure 3b using the I_{ds} vs V_{gs} curves by dividing the number of devices which have the on−off current ratio (I_{on}/I_{off}) greater than 20 by the total number of the conducting devices. In the case of TCVD, the percentage of semiconducting devices ($I_{on}/I_{off} > 20$) is almost the same for both the catalysts (Au and Fe). When it comes to the PCVD case, the Au-PCVD SWNTs display the highest concentration of the semiconducting device, which can be attributable to the high percentage of semiconducting SWNTs[21] prepared by PCVD[22] in addition to the narrow chirality distribution realized by the Au catalyst.

In conclusion, we have for the first time demonstrated the narrow-chirality distributed growth of SWNTs from the nonmagnetic catalyst. The Au catalzed PCVD growth under the appropriate hydrogen concentration is figured to be the critical factor in achieving the narrow chirality distribution. The narrow-chirality distributed SWNTs selectively grown from the nonmagnetic catalyst could be attractive to both fundamental studies of intrinsic magnetic properties of SWNTs and industrial applications to nanoelectronics.

Acknowledgment. Z.G. was supported by Tohoku University 21st Century and Global Center of Excellence (COE) Programs, Japan.

Supporting Information Available: Experimental details. Electron microscopy analysis of Au-PCVD SWNTs. PLE maps of different combinations of catalyst types and CVD methods. Raman measurement of Au-TCVD and Au-PCVD SWNTs growth. PLE maps of Au-PCVD SWNTs grown under different growth conditions. This material is available free of charge via the Internet at http://pubs.acs.org.

References

(1) Wind, S.; Appenzeller, J.; Martel, R.; Derycke, V.; Avouris, Ph. *Appl. Phys. Lett.* **2002**, *80*, 3817.
(2) Javey, A.; Guo, J.; Wang, Q.; Lundstrom, M.; Dai, H. *Nature* **2003**, *424*, 654.
(3) Dresselhaus, M. S.; Dressehaus, G.; Avouris, P., Eds. Carbon Nanotubes: Synthesis, Structure, and Applications. *Topics in Applied Physics 80*; Springer: Berlin, 2001; p 447.
(4) Tans, S. J.; Verschueren, A. R. M.; Dekker, C. *Nature* **1998**, *393*, 49.
(5) Gruner, G. *Sci. Am.* **2007**, *296*, 76.
(6) Kitiyanan, B.; Alvarez, W. E.; Harwell, J. H.; Resasco, D. E. *Chem. Phys. Lett.* **2000**, *317*, 497.
(7) Miyauchi, Y.; Chiashi, S.; Murakami, Y.; Hayashida, Y.; Maruyama, S. *Chem. Phys. Lett.* **2004**, *387*, 198.
(8) Li, X.; Tu, X.; Zaric, S.; Welsher, K.; Seo, W. S.; Zhao, W.; Dai, H. *J. Am. Chem. Soc.* **2007**, *129*, 15770.
(9) Chiang, W. H.; Sankaran, M. R. *Nat. Mater.* **2009**, *8*, 886.
(10) Zhou, W.; Han, Z.; Wang, J.; Zhang, Y.; Jin, Z.; Sun, X.; Zhang, Y.; Yan, C.; Li, Y. *Nano Lett.* **2006**, *6*, 2987.
(11) Takagi, D.; Homma, Y.; Hibino, H.; Suzuki, S.; Kobayashi, Y. *Nano Lett.* **2006**, *6*, 2642.
(12) Takagi, D.; Kobayashi, Y.; Hibino, H.; Suzuki, S.; Homma, Y. *Nano Lett.* **2008**, *8*, 3.

(13) Bhaviripudi, S.; Mile, E.; Steiner, S. A., III.; Zare, A. T.; Dresselhaus, M. S.; Belcher, A. M.; Kong, J. *J. Am. Chem. Soc.* **2007**, *129*, 1516.
(14) Ma, Y.; Lehtinen, P. O.; Foster, A. S.; Nieminen, R. M. *New J. Phys.* **2004**, *6*, 68.
(15) Kato, T.; Hatakeyama, R. *Appl. Phys. Lett.* **2008**, *92*, 031502.
(16) Jorio, A.; Pimenta, M. A.; Filho, A. G. S.; Saito, R.; Dresselhaus, G.; Dresselhaus, M. S. *New J. Phys.* **2003**, *5*, 139.
(17) Bachilo, S. M.; Strano, M. S.; Kittrel, C.; Hauge, R. H.; Smalley, R. E.; Weisman, R. B. *Science* **2002**, *298*, 2361.
(18) Yazyev, O. V.; Pasquarello, A. *Phys. Rev. Lett.* **2008**, *100*, 156102.
(19) Ding, F.; Larsson, P.; Larson, J. A.; Ahuja, R.; Duan, H.; Rosen, A.; Bolton, K. *Nano Lett.* **2008**, *8*, 463.
(20) Bachilo, S. M.; Balzano, L.; Herrera, J. E.; Pompeo, F.; Resasco, D. E.; Weisman, R. B. *J. Am. Chem. Soc.* **2003**, *125*, 11186.
(21) Liu, B.; Ren, W.; Liu, C.; Sun, C. H.; Gao, L.; Li, S.; Jiang, C.; Cheng, H. M. *ACS Nano* **2009**, *3*, 3421.
(22) Li, Y.; Mann, D.; Rolandi, M.; Kim, W.; Ural, A.; Hung, S.; Javey, A.; Cao, J.; Wang, D.; Yenilmez, E.; Wang, Q.; Gibbons, J. F.; Nishi, Y.; Dai, H. *Nano Lett.* **2004**, *4*, 317.

JA103362J